

Semiautomatic detection of coastal mangroves with Landsat Level-2

Escobar Flores, Jonathan G. 1 Sandoval, Sarahi 2*

¹ Instituto Politécnico Nacional, CIIDIR Unidad Durango, 34220, Mexico

² CONAHCYT – Instituto Politécnico Nacional, CIIDIR Unidad Durango, 34220, Mexico

* Correspondence: sarahisandoval@gmail.com

ABSTRACT

Objective: A model for rapid detection of coastal mangrove cover was devised. The idea is that it can be applied by users with basic knowledge of remote sensing and GIS.

Design/methodology/approach: The model is based on calculating the first three principal components (PC) from bands corresponding to the visible, near infrared, and shortwave infrared regions in Landsat Level-2 images. The model was tested for three RAMSAR sites located in different hydroclimatic conditions in Mexico: Laguna Guasima on the upper Gulf of California coast, Puerto Arista on the Pacific Ocean coast, and Laguna Madre on the Gulf of Mexico.

Results: It was found that the first PC in the three RAMSAR sites explains 80 to 90% of the variation and corresponds mainly to areas that include crop fields or urban infrastructure. The second PC, with cumulative variance of 8 to 14%, corresponds mainly to mangrove cover, and the PC with the lowest percentage of cumulative variance (<5.0%) is invariably open water.

Limitations on study/implications: The advantage of using Landsat Collection Level 2 is that there is an archive managed by the USGS of imagery from virtually all over the world that is over 50 years old. This model is not able to identify mangrove species.

Findings/conclusions: The advantages of this proposed model are: 1) it uses Collection 2 Level-2 images, which have radiometric and atmospheric corrections; 2) since it is carried out in ArcGIS Model Builder, it can be automated, making it intuitive and enabling the results to be exported to a Python script; and 3) the model can be replicated accurately with the QGIS model builder tool.

Keywords: Mangrove, Landsat, Remote sensing, Principal components, Mexico.

Citation: Escobar Flores, J. G., & Sandoval, S. (2025). Semiautomatic detection of coastal mangroves with Landsat Level-2. *Agro Productividad*. <https://doi.org/10.32854/c4cdpd78>

Academic Editor: Jorge Cadena Iñiguez

Associate Editor: Dra. Lucero del Mar Ruiz Posadas

Guest Editor: Daniel Alejandro Cadena Zamudio

Received: March 14, 2025.

Accepted: June 26, 2025.

Published on-line: September 9, 2025.

Agro Productividad, 18(7), July, 2025. pp: 221-230.

This work is licensed under a Creative Commons Attribution-Non-Commercial 4.0 International license.



INTRODUCTION

Mangrove swamps are among the main ecosystems that contribute to mitigation of climate change. They protect coasts from storms and soil erosion, and control flooding, and are considered to be “blue carbon” (store large amounts of carbon) due to their high rate of carbon sequestration compared to other ecosystems. Thus, they provide a diversity of ecosystem services that benefit human communities (Herrera-Silveira *et al.*, 2016; Taillardat *et al.*, 2018; Zeng *et al.*, 2023).

The remote sensing techniques available at this time seem promising for the study and monitoring of mangrove cover, but their use requires extensive knowledge in the area of remote sensing, which the relevant decision makers generally do not have. For example, Saoum and Sarkar (2024) analyzed the changes in mangrove forest dynamics over the last 20 years in Bangladesh, using Google Earth Engine (GEE) and the IDRISI program to detect forest changes with the CA-Markov model. Another example is the research of Jia *et al.* (2023), who also use GEE and algorithms such as OBIA and Random Forest to estimate the global distribution of mangrove cover. In order for users to be able to replicate this research, a background in programming, geographic information systems, remote sensing and classification algorithms would be required. Often, those who manage these lands do not have this set of skills.

Principal component analysis (PCA) is a simple technique that is easy to replicate in virtually any geographic information system. The main objective is to summarize the information contained in a group of variables into a new, smaller set without losing a significant part of the information (Chuvieco, 2019). Satellite image acquisitions in adjacent bands of the spectrum tend to detect redundant information due to the fact that different canopies on the ground present similar behavior when their electromagnetic spectrum lengths are close to each other. PCA is widely used for a variety of purposes in the study of mangrove swamps. For example, Tossi *et al.* (2022) propose a mangrove disturbance index for Iranian mangrove swamps that is generated by means of a PCA generated from WorldView-2 and Sentinel-2 multispectral images. These authors note that the advantage of using PCA over other object extraction methods are that 1) it removes correlated features, and 2) it eliminates the problem of multicollinearity (Brauner and Shacham, 2000).

This study proposes the use of images from any Landsat Collection Level-2 platform for extracting mangrove cover. The method has the advantage that the data collected are scientific products that provide images of the spectral reflectance of the Earth's surface as it would be measured at ground level in the absence of atmospheric scattering or absorption. USGS Landsat Collection 2 offers improved processing, geometric accuracy, and radiometric calibration compared to the previously available Collection 1 products.

MATERIALS AND METHODS

Three RAMSAR sites in Mexico were selected, to represent the different hydroclimatic conditions of the coasts of Mexico. The first area was Laguna Guasima, located in northern Sonora state (Figure 1a). This lagoon is dominated by mangrove swamp of the Gulf of California ecoregion, which is in the transition between tropical and subtropical climates. The Gulf is exposed to climate variability on a large scale (1200 km), including the El Niño Southern Oscillation (ENSO) and the Pacific Decadal Oscillation (Lluch-Cota *et al.*, 2013; Páez-Osuna *et al.*, 2016). The second area was Puerto Arista in the state of Chiapas (Figure 1b) a Ramsar site and also a natural protected area (sanctuary), located in the state of Chiapas. This Ramsar site has the tallest mangroves (35 m) in North America and is one of the few flooded mangrove forests in Mexico (Mendoza, 2000). The climate in this area is tropical humid (Aw) with a mean annual temperature of 28 °C and an annual precipitation of 2500 mm to 3000 mm. The vegetation around the mangrove forest is medium height

sub-evergreen forest and low sub-deciduous forest (Hernández-Hernández and Chávez, 2021). The third site is La Laguna Madre in the state of Tamaulipas (Figure 1c), another coastal mangrove swamp, on the Gulf of Mexico. This lagoon is of vital importance for the redhead (*Aythya americana*), as more than 75% of the global population of this duck spends the winter there each year (Onuf, 2007). The salinities of the lagoon are higher than those of the neighboring sea nearly all year round (Sánchez-Ramírez and Ocaña-Luna, 2015) and the main resource harvested is oysters, accounting for 79% of the extraction in Tamaulipas (Téllez *et al.*, 1999).

Landsat Level 2 data and processing

The images used in the study are from Landsat satellites and were downloaded from the United States Geological Survey (USGS) website www.earthexplorer.com. Specifically, the images used were from Landsat 9 OLI-2 (operational land imager) for Laguna Guasima, Landsat 5 TM (thematic mapper) for La Laguna Madre, and Landsat 8 OLI for Puerto Arista with date of acquisition in cloud-free months and before the rains

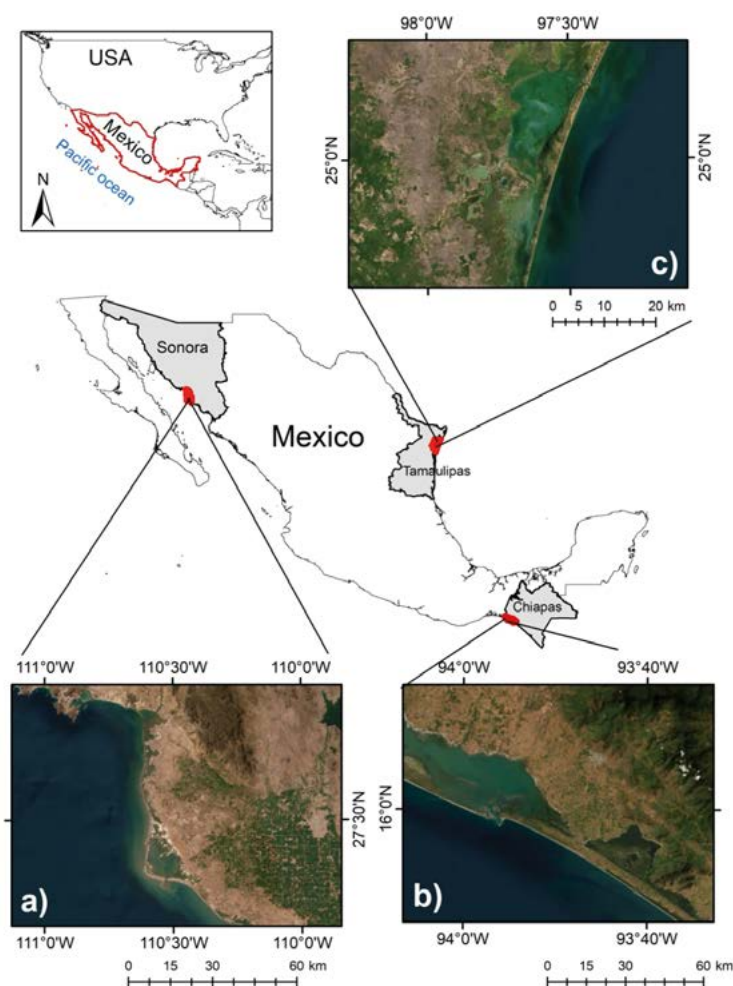


Figure 1. Study areas: Ramsar wetlands in coastal regions of Mexico. 1a. Laguna Guasima, Sonora, 1b. Puerto Arista, Chiapas, 1c. Laguna Madre, Tamaulipas in Mexico.

(Téllez *et al.*, 1999; Hernández-Hernández and Chávez, 2021) (Table 1). The purpose of using different Landsat products is to determine whether the different radiometric resolutions affect the PCA result, and if not, then users can conduct multitemporal analyses with these Landsat products.

The spectral bands of these images have temporal consistency within the same band and are therefore suitable for comparison purposes (Wulder *et al.*, 2016; Teixeira *et al.*, 2020).

The images are from Collection 2 Level-2, which have the advantage of being radiometrically calibrated and have high precision orthorectification using ground control points and a digital elevation model (DEM). In addition, the images had been atmospherically corrected by the Landsat Ecosystem Disturbance Adaptive Processing System (LEDAPS, version 3.4.0) for Landsat 5-7 and the Landsat Surface Reflectance Code (LaSRC, version 1.5.0) for Landsat 8 and 9 (USGS Landsat Science Products, <https://www.usgs.gov/landsat-missions/landsat-science-products>) (Vogelmann *et al.*, 2016).

To obtain the bands in TOA (top of the atmosphere) values for both TM and OLI sensors, users of Level-2 imagery need only multiply by the scaling factor and subtract the additive factor as shown in the following Equation (1).

$$TOA\ Reflectance = (band * 0.0000275) + (-0.2) \quad \text{Eq. 1}$$

Using PCA in ArcGIS

The model builder in ArcGIS was used to carry out an automatization process to extract both mangrove cover polygons. This tool has the advantage that it can be exported to a

Table 1. Bands from Landsat level 2 satellite data for each of the three study locations.

Area	Date of acquisition	Sensor	Radiometric resolution	Spectral bands used (micrometers)	Resolution (meters)
Laguna Guasima	April 7, 2024	Landsat 9- OLI 2	14 bits	Band 2 (0.45-0.51) Band 3 (0.53-0.59) Band 4 (0.64-0.67) Band 5 (0.85-0.88) Band 6 (1.57-1.65) Band 7 (2.11-2.29) Band 10 (10.6-11.19)	30
Puerto Arista	April 4, 2023	Landsat 8-OLI	12 bits	Band 2 (0.45-0.51) Band 3 (0.53-0.59) Band 4 (0.64-0.67) Band 5 (0.85-0.88) Band 6 (1.57-1.65) Band 7 (2.11-2.29) Band 10 (10.6-11.19)	30
Laguna Madre	May 10, 1993	Landsat 5-TM	8 bits	Band 1 (0.45-0.52) Band 2 (0.52-0.60) Band 3 (0.63-0.69) Band 4 (0.76-0.90) Band 5 (1.55-1.75) Band 6 (10.4-12.5) Band 7 (2.08-2.35)	30

Python script. The first step is to scale the atmospherically corrected bands to be used in the principal component analysis (PCA). These bands correspond to the visible, near infrared, and mid-wave infrared regions of the electromagnetic spectrum Atmospheric correction is already provided for each of the Landsat image bands from Collection Level-2, so it is only necessary to convert the values to TOA. The next step is to delimit the bands to the area of interest (Ramsar sites) so that all bands can be included in the PCA. The PCA process in ArcGIS basically consists of the following: 1) calculate the variance–covariance matrix of the spectral bands, 2) extract the eigenvalues that represent the magnitude of the vector of each successive component, and 3) produce a raster with the components that retain the information (Figure 2).

Extraction of mangrove

The PCA raster was reclassified following the Jenks natural breaks method (Jenks, 1997), whose main objective is to generate homogeneous groups that maximize the variance between class means and minimize the variance within classes (Chen *et al.* 2013). This procedure is carried out with the Reclassify function in ArcGIS (Figure 2). Three classes were defined, which correspond to the first three components, which contain the highest variance in a multispectral image (Chuvieco, 2019). The result of the reclassification was an integer raster containing integer values of 1 for pixels corresponding to PC1; values of 2 for PC2 pixels, a principal component which has been reported to have a close relationship with dense vegetation areas (Estornell *et al.*, 2012) and mangroves (Sunkur *et al.*, 2023); and values of 3 for PC3, which corresponds to pixels with low multispectral variability, which

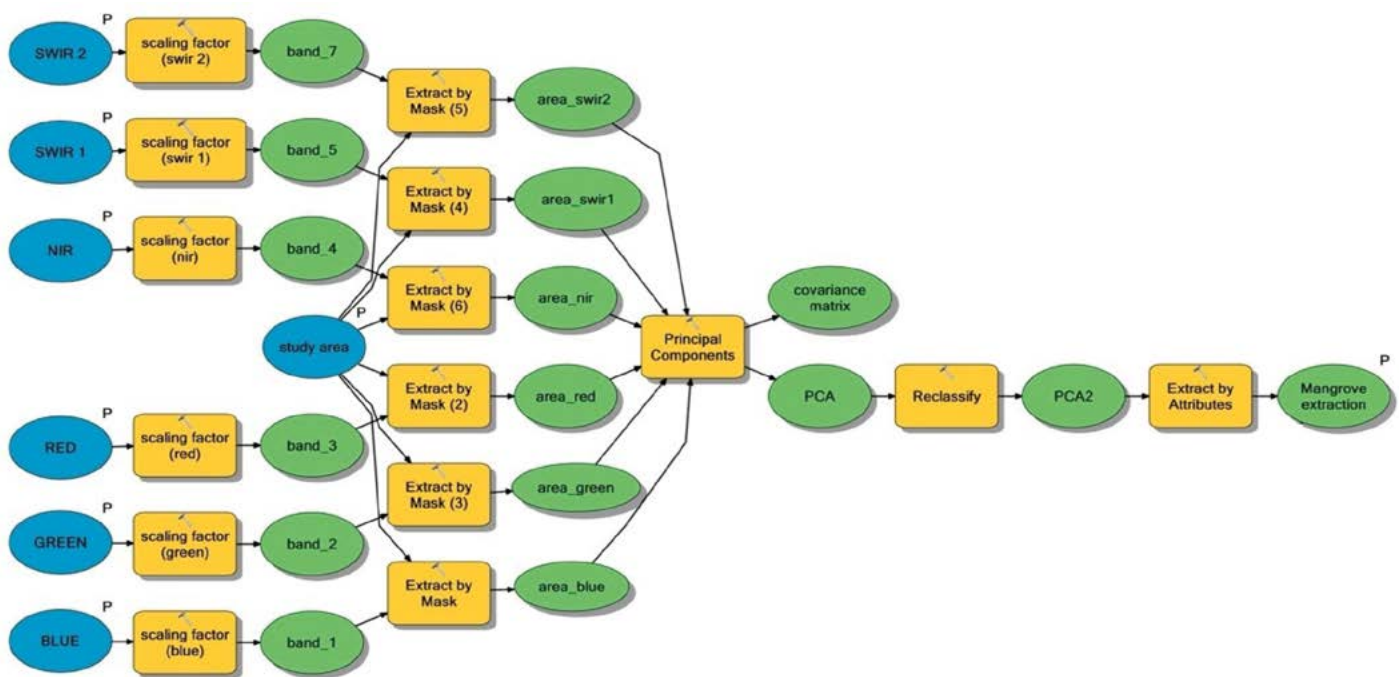


Figure 2. Automation model for extraction of mangrove cover and corresponding LST values. Blue ovals have a P superscript indicating that users only have to load the spectral bands of their site of interest. Yellow squares are geospatial processes and green ovals are the result of each geoprocess.

has been reported to be related to water bodies (Balázs *et al.*, 2018). Pixel classification by Jenks's method has proven to be useful for mangrove classification when using spectral bands from satellite images (Nuarsa *et al.*, 2010).

RESULTS AND DISCUSSION

In all Ramsar sites, mangrove cover was clearly delimited in PC 2 with cumulative variances of 3% to 14%. The mangrove swamp with the lowest percentage of variance was Laguna Guasima (Table 2, Figure 3). PC 3 for the three sites had cumulative variance of less than 5% and in the images always corresponded to bodies of surface water (Table 2, Figure 2), while PC 1 ranged from 80% to 92% of cumulative variance for the three sites and corresponded to areas of cropland, urban land, and vegetation (Table 2, Figure 3). For the eigenvectors of PC 2 it was found that in Laguna Madre the spectral band that made the greatest contribution was the NIR, while for Puerto Arista it was SWIR 1 and SWIR 2, and for Laguna Guasima it was the red and green bands (Table 2). In PC 1 all eigenvectors were positive and the highest values were found in the SWIR bands for all three areas (Table 3). In PC 3, in Laguna Madre and Puerto Arista the eigenvector with the highest value was in the red band while for Puerto Arista it was the NIR band (Table 3).

PCA is a multivariate statistical technique that is very useful in remote sensing because it reduces the dimensionality of the spectral bands (Harsanyi and Chang 1994). For example, in our study, transforming the multispectral images composed of three visible bands, one near infrared and two mid-wave infrared, resulted in a set of uncorrelated bands (orthogonal) that facilitated the detection of mangrove cover and water bodies. The detection of mangrove cover in PC 2 coincides with the detection of dense vegetation areas in other investigations such as in Valencia, Spain (Estornell *et al.* 2012). For the case of mangrove cover in Puerto Arista, the eigenvector value of the infrared band is indeed the highest (Table 3). PCA is considered one of the most efficient methods for mangrove cover detection; for example, Green *et al.* (1998) mapped mangrove cover in the Turks and Caicos Islands using various sensors; Landsat, SPOT, and Compact Airborne Spectrographic Imager. They tested different classification methods, from visual interpretation to supervised and unsupervised classification and concluded that PCA has up to 92% accuracy. Once again, the eigenvalues of NIR and red were the

Table 2. Cumulative variances obtained for the first 3 PCA in the study areas.

Ramsar site	Sensor and date	Ocean	Cumulative variance (%) and principal land cover
Laguna Guasima	Landsat 9 OLI 2 07/04/2024	Gulf of California	PCA 1=92.79 Ground PCA 2=3.94 Mangrove PCA 3=2.75 Water
Puerto Arista	Landsat 8 OLI 05/04/2023	Pacific Ocean	PCA 1=88.96 Ground PCA 2=8.87 Mangrove PCA 3=1.90 Water
Laguna Madre	Landsat 4 TM 03/10/1993	Gulf of México	PCA 1=80.30 Ground PCA 2=14.13 Mangrove PCA 3=5.00 Water

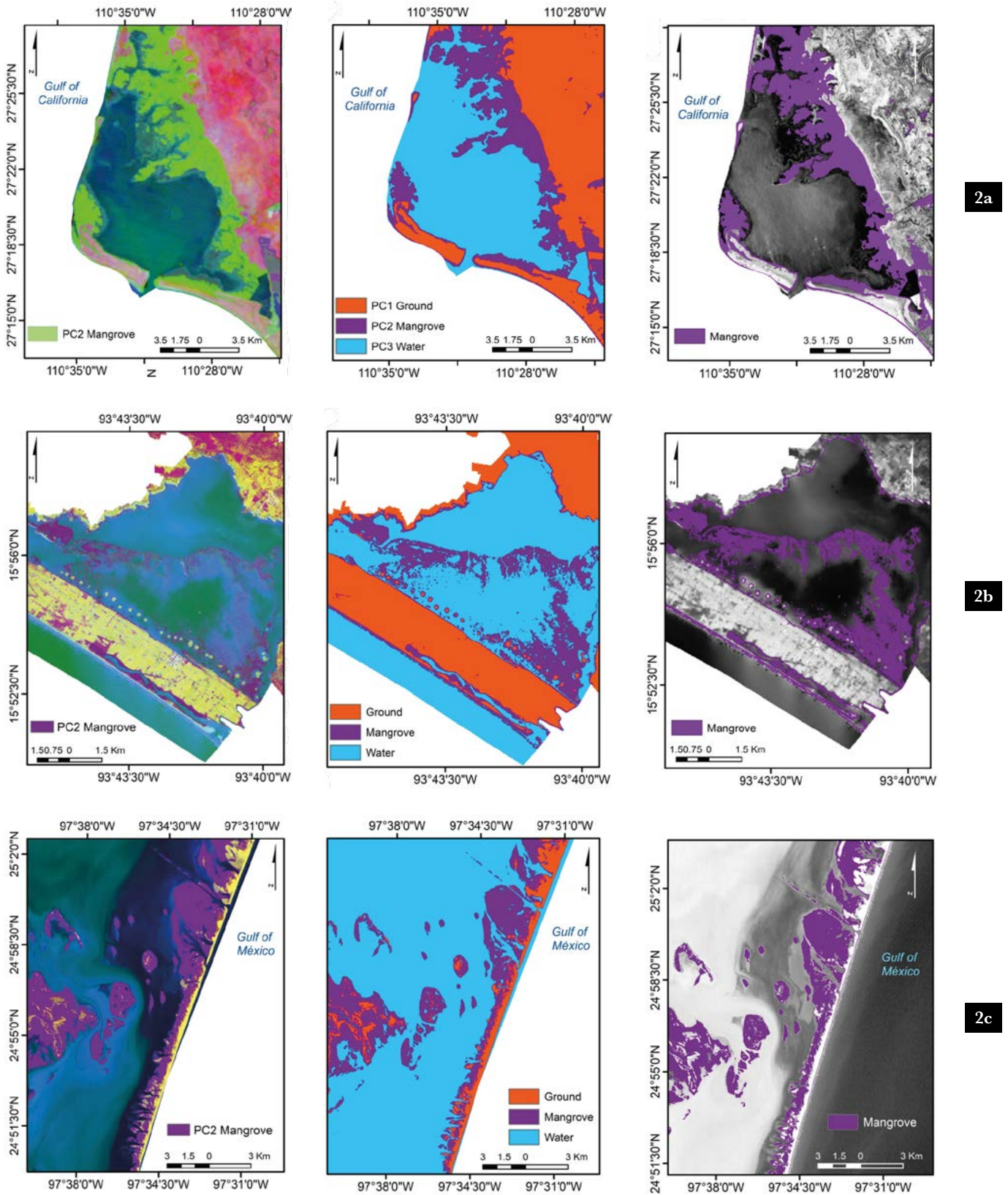


Figure 3. Studied mangrove swamps on Mexican coasts; 2a) Laguna Guasima, Sonora; 2b) Puerto Arista, Chiapas; 2c) Laguna Madre, Tamaulipas.

Table 3. Values of eigenvectors obtained for the first 3 PCs of the study areas.

Mangrove	Band	PCA1	PCA2	PCA3
Laguna Guasima	SWIR-1	0.543	-0.200	-0.528
	SWIR-2	0.576	-0.277	-0.166
	NIR	0.431	-0.259	0.829
	Red	0.292	0.552	0.027
	Green	0.292	0.552	0.027
	Blue	0.126	0.453	0.073
Puerto Arista	SWIR-1	0.324	0.459	-0.182
	SWIR-2	0.585	0.445	-0.366
	NIR	0.721	-0.664	0.152
	Red	0.140	0.259	0.594
	Green	0.085	0.173	0.481
	Blue	0.084	0.231	0.475
Laguna Madre	SWIR-1	0.521	-0.347	-0.150
	SWIR-2	0.680	-0.022	-0.459
	NIR	0.442	0.766	0.443
	Red	0.205	-0.391	0.451
	Green	0.129	-0.277	0.480
	Blue	0.107	-0.249	0.369

highest in PC 2. A similar pattern in cumulative variance was found to that reported by Sunkur *et al.*, (2023) in mangrove cover in Madagascar, but they use Sentinel-2 satellite images, finding cumulative variances for PC 2 between 5% and 8%, which is similar to the variances reported in this study (Table 2). PCA, besides being useful for mangrove cover detection (Kuenzer *et al.*, 2011) can also be used for change detection as reported by Prerna *et al.* (2015) in their investigation of mangrove swamp in the Gulf of Kachchh. Here, in addition to extracting mangrove cover with PCA, it was possible to identify dense and sparse mangroves, and to detect an increase in cover, from 30.69 km² in 1999 to 38.81 km² in 2010.

The advantage of using Landsat Collection Level 2 is that there is an archive managed by the USGS of imagery from virtually all over the world that is over 50 years old. Collection 2 images have better geolocation as well as radiometric calibration (Landsat 5, 8, 9) and contain global surface reflectance and surface temperature bands, which allows for multi-temporal analyses (Crawford *et al.*, 2023). Another advantage of Collection 2 is the atmospheric correction; traditional algorithms were based on dark objects and assumed that the TOA spectral reflectance of an object was equal to atmospheric reflectance (Chavez, 1996); however, these algorithms did not correct for atmospheric variations such as scattering and absorption captured by the image. In contrast, the surface reflectance obtained from Collection 2 Level-2 images is atmospherically corrected with the Landsat Ecosystem Data Adaptive Processing System (LEDAPS) algorithm (Masek *et al.*, 2006). This algorithm uses the solar spectrum vector (6SV) by band and retrieves the aerosol

optical thickness (AOT) independently using a dense and dark vegetation (DDV) approach (Crawford *et al.*, 2023).

CONCLUSIONES

This paper proposes a practical geoprocessing model for identifying and measuring mangrove cover using principal component analysis (PCA). The advantages of this method are: 1) it proposes the use of Collection 2 Level-2 images, which have radiometric and atmospheric corrections, 2) implementing the model in ArcGIS Model Builder enables an automated model that is intuitive, and allows the results to be exported to a Python script, and 3) the model can be replicated accurately with the QGIS model builder tool.

REFERENCES

- Balázs B, Bíró T, Dyke G, Kumar SS, Szabó S (2018) Extracting water-related features using reflectance data and principal component analysis of Landsat images. *Hydrological Sciences Journal*. 63(2): 269-284. <https://doi.org/10.1080/02626667.2018.1425802>
- Brauner N, Shacham M (2000) Considering precision of data in reduction of dimensionality and PCA. *Comput Chem Eng* 24(12):2603-2611. [https://doi.org/10.1016/S0098-1354\(00\)00616-5](https://doi.org/10.1016/S0098-1354(00)00616-5)
- Chavez Jr PS (1996) Image-based atmospheric corrections —revisited and improved. *Photogramm. Eng Rem Sens* 62:1025–1036.
- Chen J, Yang ST, Li HW, Zhang B, Lv JR (2013). Research on geographical environment unit division based on the method of natural breaks (Jenks). The International Archives of the Photogrammetry. *Remote Sensing and Spatial Information Sciences*, 40: 47–50.
- Chuvieco E (2019) Teledetección ambiental: La observación de la Tierra desde el espacio. Ariel.
- Crawford CJ, Roy DP, Arab S, Barnes C, Vermote E, Hulley G, Gerace A, Choate M, Engebretson C, Micijevic E, Shmidt G, Anderson C, Anderson M, Bouchard M, Cook B, Dittmeier R, Howard D, Jenkerson C, Kim M, Kleyians T, Zahn S (2023) The 50-year Landsat collection 2 archive. *Science of Remote Sensing*, 8:100103. <https://doi.org/10.1016/j.srs.2023.100103>
- Estornell J, Ruiz LA, Velázquez-Martí B, Herмосilla T (2012) Estimation of biomass and volume of shrub vegetation using LiDAR and spectral data in a Mediterranean environment. *Biomass and Bioenergy* 46:710-721. <https://doi.org/10.1016/j.biombioe.2012.06.023>
- Green EP, Mumby PJ, Edwards AJ, Clark CD, Ellis AC (1998) The assessment of mangrove areas using high resolution multispectral airborne imagery. *Journal of Coastal Research*. 14(2):433-443. <https://www.jstor.org/stable/4298797>
- Harsanyi JC, Chang CI (1994) Hyperspectral image classification and dimensionality reduction: an orthogonal subspace projection approach. *IEEE TGARS* 32:779-785. <https://doi.org/10.1109/36.298007>
- Hernández-Hernández JC, Chávez C (2021) Inventory of medium-sized and large mammals in La Encrucijada Biosphere Reserve and Puerto Arista Estuarine System, Chiapas, Mexico. *Check List*, 17:1155-1170. <https://doi.org/10.15560/17.4.1155>
- Herrera-Silveira JA, Camacho-Rico, A, Pech E, Pech M, Ramírez-Ramírez J, Teutli-Hernández C (2016) Dinámica del carbono (almacenes y flujos) en manglares de México. *Terra latinoamericana*, 34:61-72.
- Jenks GF (1977). Optimal data classification for choropleth maps. Occasional paper No. 2. Lawrence, Kansas: University of Kansas, Department of Geography
- Jia M, Wang Z, Luo L, Zhang R, Zhang H (2023). Global status of mangrove forests in resisting cyclone and tsunami. *The Innovation Geoscience* 1:100024. <https://doi.org/10.59717/j.xinn-geo.2023.100024>
- Kuenzer C, Bluemel A, Gebhardt S, Quoc TV, Dech S (2011) Remote sensing of mangrove ecosystems: A review. *Remote Sens* 3(12):878-928. <https://doi.org/10.3390/rs3050878>
- Lluch-Cota SE, Tripp-Valdez M, Lluch-Cota DB, Lluch-Belda D, Verbesselt J, Herrera-Cervantes H, Bautista-Romero JJ (2013). Recent trends in sea surface temperature of Mexico. *Atmósfera*, 26:537-546.
- Malakar N, Hulley G, Hook S, Laraby K, Cook M, Schott J (2018) An Operational Land Surface Temperature Product for Landsat Thermal Data: Methodology and Validation. *IEEE Transactions on Geoscience and Remote Sensing*, 56(10)1-19. <https://doi.org/10.1109/TGRS.2018.2824828>
- Masek JG, Vermote EF, Saleous NE, Wolfe R, Hall FG, Huemmrich KF, Gao F, Kutler J, Lim TK (2006) A Landsat surface-reflectance dataset for North America. 1990–2000: *IEEE Geoscience and Remote Sensing Letters*, 3(1):68-72. <https://doi.org/10.1109/LGRS.2005.857030>

- Mendoza OE (2000) Support of the project to protect and conserve sea turtles in “La Encrucijada” Biosphere Reserve, Chiapas, México. In: Mosier A, Allen F, Beth B (Eds.) Proceedings of the Twentieth Annual Symposium on Sea Turtle Biology and Conservation. NOAA Tech Memo. NMFS-SEFSC, Orlando, Florida, USA. 340-342.
- Nuarsa IW, Adnyana IWS, Sugimori Y, Kanno S, Nishio F (2010) Development of The New Algorithm for Mangrove Classification. *International Journal of Remote Sensing and Earth Sciences (IJReSES)*, 2:57-64.
- Onuf C (2007) Laguna Madre. In: Handley L, Altsman D, DeMay R. Seagrass Status and Trends in the Northern Gulf of Mexico: 1940–2002: U.S. Geological Survey Scientific Investigations Report, 2006–5287.
- Páez-Osuna F, Sanchez-Cabeza JA, Ruiz-Fernández AC, Alonso-Rodríguez R, Piñón-Gimate A, Cardoso-Mohedano JG, Flores-Verdugo FJ, Carballo JL, Cisneros-Mata MA, Álvarez-Borrego S (2016) Environmental status of the Gulf of California: A review of responses to climate change and climate variability. *Earth-Science Reviews*, 162:253-268. <https://doi.org/10.1016/j.earscirev.2016.09.015>
- Prerna R, Naidu V, Sukumaran S, Gajbhiye S (2015) Observed decadal changes in extent of mangroves and coral reefs in southern Gulf of Kachchh using principal component analysis and geo-spatial techniques: a case study. *Journal of Coastal Conservation*, 19(3):257-267. <https://link.springer.com/article/10.1007/s11852-015-0385-9>
- Sánchez-Ramírez M, Ocaña-Luna A (2015) Estructura y variación estacional de la comunidad ictioplanctónica en una laguna hipersalina del oeste del Golfo de México: Laguna Madre, Tamaulipas. *Hidrobiológica*, 25:175-186.
- Saoum MR, Sarkar, KS (2024) Monitoring mangrove forest change and its impacts on the environment, Ecological Indicators, 159:111666. <https://doi.org/10.1016/j.ecolind.2024.111666>
- Sunkur R, Kantamaneni K, Bokhoree C, Ravan S (2023) Mangroves’ role in supporting ecosystem-based techniques to reduce disaster risk and adapt to climate change: A review. *Journal of Sea Research*, 196: 102449. <https://doi.org/10.1016/j.seares.2023.102449>
- Taillardat P, Friess DA, Lupascu M, (2018) Mangrove blue carbon strategies for climate change mitigation are most effective at the national scale. *Biol Lett*, 14:20180251. <https://doi.org/10.1098/rsbl.2018.0251>
- Teixeira PC, Jing X, Leigh L (2020) Evaluation analysis of Landsat level-1 and level-2 data products using in situ measurements. *Remote sensing* 12(16):2597. <https://doi.org/10.3390/rs12162597>
- Téllez SJ, Oliva M, de León JR, Vázquez M (1999) Evaluación de la calidad microbiológica del ostión de “la laguna madre” de Tamaulipas (México) evaluación da calidade microbiolóxica do ostión de “la laguna madre” de Tamaulipas (México) evaluation of microbiological quality of oyster from “la laguna madre” of Tamaulipas (México). *CYTA: Journal of Food* 2:152-157. <https://doi.org/10.1080/11358129909487597>
- Tossi NB, Soffianian AR, Waser LT (2022) Mapping disturbance in mangrove ecosystems: Incorporating landscape metrics and PCA-based spatial analysis. *Ecological Indicators* 136:108718. <https://doi.org/10.1016/j.ecolind.2022.108718>
- Vogelmann J, Gallan T A, Hu S, Zhe Z (2016) Perspectives on monitoring gradual change across the continuity of Landsat sensors using time-series data. *Remote Sensing of Environment*, 185:258-270. <https://doi.org/10.1016/j.rse.2016.02.060>
- Wulder MA, White JC, Loveland TR, Woodcock CE, Belward AS, Cohen WB, Fosnight EA, Shaw J, Masek JG, Roy DP (2016) The global Landsat archive: Status, consolidation, and direction Remote Sens Environ 185:271-283. <https://doi.org/10.1016/j.rse.2015.11.032>
- Zeng J, Ai B, Jian Z, Ye M, Zhao J, Sun S (2023) Analysis of mangrove dynamics and its protection effect in the Guangdong-Hong Kong-Macao Coastal Area based on the Google Earth Engine platform. *Frontiers in Marine Science* 10:1170587. <https://doi.org/10.3389/fmars.2023.1170587>